

RESEARCH ARTICLE | DECEMBER 20 2006

Optical polarization anisotropy and hole states in pyramidal quantum dots

K. F. Karlsson; V. Troncale; D. Y. Oberli; A. Malko; E. Pelucchi; A. Rudra; E. Kapon



Appl. Phys. Lett. 89, 251113 (2006)

<https://doi.org/10.1063/1.2402241>

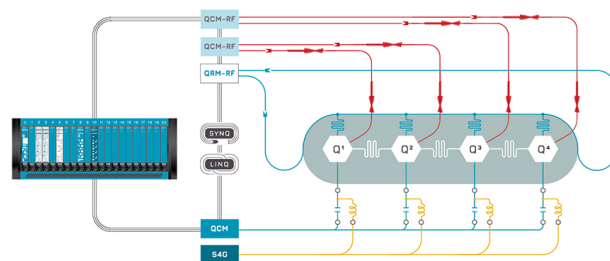


CrossMark



Integrates all
Instrumentation + Software
for Control and Readout of

Superconducting Qubits
NV-Centers
Spin Qubits



Superconducting Qubit Setup

[find out more >](#)

Optical polarization anisotropy and hole states in pyramidal quantum dots

K. F. Karlsson,^{a)} V. Troncale, D. Y. Oberli, A. Malko,^{b)} E. Pelucchi, A. Rudra, and E. Kapon
Laboratory of Physics of Nanostructures, Ecole Polytechnique Fédérale de Lausanne (EPFL), CH-1015 Lausanne, Switzerland

(Received 29 August 2006; accepted 19 October 2006; published online 20 December 2006)

The authors present a polarization-resolved photoluminescence study of single semiconductor quantum dots (QDs) interconnected to quantum wires, measured both in a top geometry, and in a less conventional cleaved-edge geometry. Strong polarization anisotropy is revealed for all observed transitions, and it is deduced that closely spaced QD hole states exhibit nearly pure heavy-or-light-hole character. These effects are attributed to the large aspect ratio of the dot shape. © 2006 American Institute of Physics. [DOI: 10.1063/1.2402241]

Semiconductor quantum dots (QDs) have unique atomic-like optical properties, which makes them highly interesting for use as the active material in optoelectronic devices such as single photon emitters and lasers. In this context, the QD light emission pattern and its polarization state are of vital importance. However, spectroscopic studies on semiconductor QDs have mainly been performed in a top geometry where the luminescence is extracted along the growth direction. Information on the polarization of the emission is then limited to the polarization state in the plane of the sample. Indeed, in-plane polarization anisotropy of excitonic features has been widely studied for single QDs in various materials systems such as GaAs/AlGaAs, CdSe/ZnSe, and InAs/GaAs.¹⁻³ Mostly studied are Stranski-Krastanow (SK) InAs/GaAs QDs, grown on (001) substrates, which possess C_{2v} symmetry. The low symmetry of such QDs has been evidenced by in-plane anisotropy of the luminescence from the ground state transitions in single SK QDs (Ref. 4) as well as ensembles.^{5,6} However, only a few studies have been devoted to the vertical polarization state, which can be probed from the side of the sample. The main direction of linear polarization of the edge emission strongly depends on the QD capping material,⁷ and it can be altered by vertical coupling in stacked QDs.⁸ The reported measurements were performed on SK QD ensembles, which suffer from substantial inhomogeneous broadening full width half maximum (>40 meV) concealing the detailed structure. Very recently this problem was overcome by cleaved-edge measurements on single SK QDs, resolving the exciton fine structure for which strong in-plane polarization was demonstrated.⁹ However, only emission from the QD ground state was studied in that work.

In this letter, we discuss both in-plane and vertical polarization dependence of the photoluminescence (PL) from single pyramidal InGaAs/AlGaAs QDs. Optical transitions related to the ground and the excited QD levels as well as the AlGaAs quantum wire (QWR) barrier are studied. It is experimentally shown that these QDs exhibit isotropic in-plane linear polarization dependence, while strong and different polarization dependencies are observed from the cleaved edge. From these data, the degree of valence band mixing is quantified.

The investigated semiconductor QDs were grown by low-pressure organometallic chemical vapor deposition on 2° off-(111)*B* GaAs substrates prepatterned with a $5\ \mu\text{m}$ pitch array of inverted tetrahedral pyramids.¹⁰ The sample was produced by growing the following layer sequence: 45 nm thick $\text{Al}_{0.75}\text{Ga}_{0.25}\text{As}$ layer, 130 nm $\text{Al}_{0.55}\text{Ga}_{0.45}\text{As}$, 70 nm $\text{Al}_{0.3}\text{Ga}_{0.7}\text{As}$, a 0.5 nm $\text{In}_{0.1}\text{Ga}_{0.9}\text{As}$ quantum well (QW) layer, 70 nm $\text{Al}_{0.3}\text{Ga}_{0.7}\text{As}$, and 130 nm $\text{Al}_{0.55}\text{Ga}_{0.45}\text{As}$. Thicknesses refer to growth on a planar (100) substrate. The layers were nominally undoped. Growth on the nonplanar substrate yields a lens-shaped InGaAs QD at the bottom of the inverted pyramid. In addition, a vertical AlGaAs QWR (VQWR) is formed in the growth direction along the vertical axis of the pyramid, due to Al-Ga segregation.¹¹ The inset of Fig. 1(a) illustrates schematically such pyramidal QD inter-

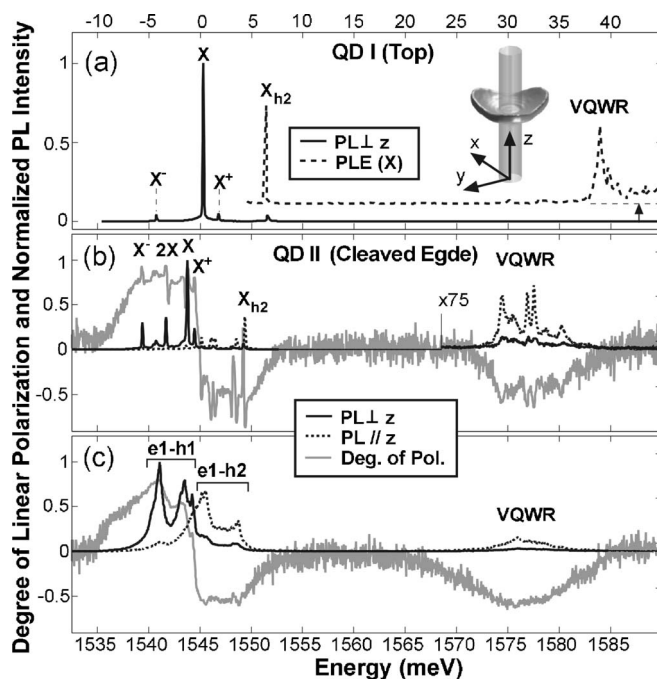


FIG. 1. (a) μPL and μPLE (vertically shifted) spectra of QD I measured in top geometry using excitation powers of 1.25 nW and 4 μW , respectively. [(b) and (c)] Polarization-resolved μPL spectra with extracted degree of linear polarization P of QD II measured in cleaved-edge geometry at moderate and high excitation powers of 45 and 90 nW, respectively. The upper (lower) horizontal axis indicates the relative (absolute) photon energy. The inset in (a) schematically illustrates the QD and the VQWR oriented along the z direction.

^{a)}Electronic mail: fredrik.karlsson@epfl.ch

^{b)}Present address: Los Alamos National Laboratory, Center for Integrated Nanotechnologies, MPA-CINT, MS G755, Los Alamos, NM 87545.

sected by the VQWR, where z indicates the $[111]$ growth direction and x (y) is the $[\bar{1}10]$ ($[11\bar{2}]$) crystallographic direction. By this choice of growth axis, the pyramidal QDs possess C_{3v} symmetry, which implies higher symmetry of the QD shape, strain fields, and the piezoelectric potential as compared with SK QDs.¹²

The optical emission properties of single pyramidal QDs were studied experimentally using a conventional micro-PL (μ PL) and μ PL-excitation (μ PLe) setups. The sample was mounted in a He-flow cryostat and kept at a constant temperature chosen in the range of 10–35 K in order to avoid thermal excitation and maximize the optical efficiency. The pyramids containing the QDs were optically excited by a frequency-doubled diode-pumped Nd:YVO4 laser at 532 nm wavelength for nonresonant μ PL and by a tunable cw Ti:sapphire laser for μ PLe. The spatial resolution was $\sim 1 \mu\text{m}$ and the spectral resolution was set at $120 \mu\text{eV}$. A linear polarizer was mounted in front of the spectrograph entrance at fixed polarization direction, and the slow axis of a preceding $\lambda/2$ plate was rotated in order to resolve the linear polarization content of the incident signal.

The polarization characteristics of several single QDs were measured, all exhibiting the same features. Typical data of three QDs (QDs I–III) are presented here, all having identical excitonic transitions with small ($<0.5 \text{ meV}$) relative differences in transition energies. Excellent spectral reproducibility from QD to QD is a general property of pyramidal QDs.¹⁰ QD I was processed for maximal light extraction required for μ PLe measurements by substrate removal and was optically accessed from the tip of the pyramid.¹³ The polarization measurements were performed on “as grown” QD II and QD III, optically accessed from the sample cleaved-edge and from the top (base of pyramid), respectively.

A typical μ PL spectrum of QD I recorded in the top-geometry configuration is reported in Fig. 1(a) (solid line). The single exciton (X) dominates the spectrum, but by changing the excitation power or crystal temperature the charge state of the QD can be tuned^{14–16} in a well-controlled way and the intensity of the negatively or positively charged excitons (X^- or X^+) may overtake that of X . At higher excitation powers also contribution of the biexciton ($2X$) appears. These excitonic transitions, which in a single-particle picture are all related to the QD’s electron and hole ground states ($e1-h1$), are well understood for this system as established by a complete set of second-order auto- and cross-correlation measurements.¹⁴ The QDs were designed to have only one confined electron level, which is reflected to by the absence of spectral lines from multinegatively charged excitons.¹⁶ Besides X^+ , additional spectral features can be observed on the high-energy side of X , typically up to 7 meV above the X emission. Such features *always* exhibit very weak PL emission in comparison to the dominating one(s) of X , $2X$, X^- , or X^+ for this top-geometry configuration. A corresponding resonance (X_{h2}) is revealed in the μ PLe spectrum of the X emission shown in Fig. 1(a) (dotted line). Notably, no additional PLe resonance is observed up to the excitation of the VQWR starting at 30–40 meV above the X emission. Since the VQWR is physically connected to the QD, it is expected that the carriers photogenerated in the VQWR are efficiently transferred to the QD before recombining there.¹⁴ Consequently, X_{h2} is the sole observed excited optical resonance in

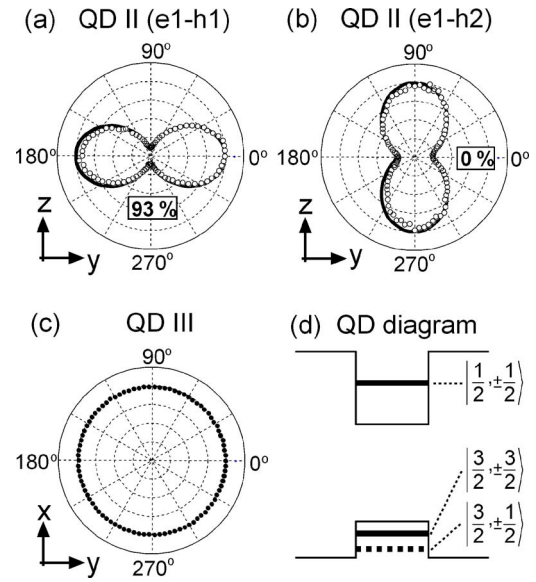


FIG. 2. Linear polarization dependence of the QD ground (a) and excited (b) emissions in the yz plane and the total QD emission (c) in the xy plane. The black solid lines in (a) and (b) are the squared dipolar matrix elements corresponding to $HH=93\%$ and $HH=0\%$ heavy-hole character. Excitation powers of 45 and 150 nW were used to excite QD II and QD III in [(a) and (b)] and (c), respectively. A diagram of the QD states is shown in (d) with energy levels denoted $|J, J_z\rangle$.

the QD. It is attributed to a transition involving the ground electron and a hole in the second energy state with finite electron-hole wave function overlap integral ($e1-h2$).

Measurements in top-view configuration do not reveal any in-plane polarization anisotropy of the observed spectral features. The full angular dependence of the integrated QD intensity is shown in Fig. 2(c). This profile is independent of integration region and in Fig. 2(c) the total QD emission was integrated.

For measurements in side-view configuration, the samples were cleaved along $[11\bar{2}]$ (y) and the emission was collected along the $[\bar{1}10]$ (x) direction. In this way, the polarization anisotropy in the yz plane could be probed. The corresponding PL spectra of QD II are shown in Figs. 1(b) and 1(c), for moderate and high excitation powers, respectively. Strong anisotropy is detected for polarizations oriented parallel (dashed lines) and perpendicular (solid black lines) to z . The VQWR emission at $\sim 1575 \text{ meV}$ is enhanced when detecting along z , parallel to the VQWR, as expected.^{17,18} The emission originates from electron-hole pairs trapped in localized states of the VQWR, and the VQWR emission band is Stokes shifted with respect the μ PLe [Fig. 1(a)] by $\sim 7 \text{ meV}$. Furthermore, parallel detection almost completely suppresses the contribution of the QD ground emission ($e1-h1$), while a strong enhancement of the QD excited emission ($e1-h2$) is observed. This effect is more clearly seen in the degree of linear polarization P plotted as solid gray lines in Figs. 1(b) and 1(c), where $P=(I_y-I_z)/(I_y+I_z)$ and $I_{y,z}$ is the detected intensity for a polarization directions along y or z . For the ground emission P is near unity [see Fig. 1(b)], but at certain energy P abruptly switches sign and essentially remains negative up to the VQWR energy. The energy at which this switching occurs is located between the highest ground emission and the lowest excited emission energies. This clearly demonstrates that the ground state

emission ($e1-h1$) has a unique direction of polarization, different from other emission bands in this system. For increased excitation power, the strong polarization anisotropy holds [Fig. 1(c)] and is only slightly reduced near the switching energy due to line broadening effects.

The squared dipolar matrix element for optical transitions between electrons in the conduction band ($J=1/2$) and holes in the valence band ($J=3/2$) may exhibit polarization anisotropy due to the two different hole character types.¹⁹ The heavy and light holes are distinguished by the angular momentum projection (J_z) on a quantization axis (z), for which $J_z = \pm 3/2$ and $J_z = \pm 1/2$, respectively. An anisotropic confinement potential, e.g., caused by a quantum structure, can remove the degeneracy of these levels and possibly mix them. The degree of valence band mixing determines the polarization anisotropy. Pure heavy- and light-hole states of different energy are realized in QWs. However, in QWRs and QDs, some degree of valence band mixing may occur, and the polarization anisotropy is reduced and vanishes in the limit of complete mixing in perfectly isotropic QDs. For a system that is isotropic in linear polarization in the plane perpendicular to z , the intensity I of light linearly polarized with an angle $(\pi/2 - \alpha)$ with respect to the z axis is^{18,19}

$$I \propto \left(\frac{1}{2} |J_{3/2}|^2 + \frac{1}{6} |J_{1/2}|^2 \right) \cos^2(\alpha) + \frac{2}{3} |J_{1/2}|^2 \sin^2(\alpha), \quad (1)$$

where

$$|J_m|^2 = \sum_{l=-m,n} |\langle \varphi^{CB} | \varphi_i^{VB} \rangle|^2 \quad (2)$$

and φ^{CB} (φ^{VB}) is the electron (hole) envelope wave function. In order to quantify the degree of valence band mixing, the parameter $HH = |J_{3/2}|^2 / (|J_{1/2}|^2 + |J_{3/2}|^2)$ will be used, for which 100% (0%) correspond to pure heavy (light) character for the hole overlapping with the electron.

Since no polarization anisotropy was observed for our QDs in the xy plane, the growth direction $[111]$ (z) is here the appropriate choice of quantization axis. Thus, values of HH for the QD transitions can be estimated from the experimental data. The full yz -plane angular dependence of linear polarization was obtained by integrating the QD intensity in the measured spectra over the two spectral regions for which the degree of polarization is positive or negative, respectively. The result is represented by polar plots in Figs. 2(a) and 2(b) (circles). The corresponding theoretical polarization dependences $I(\alpha)$ of the squared dipolar matrix elements corresponding to $HH=93\%$ and $HH=0\%$ are plotted as solid black lines in Figs. 2(a) and 2(b), respectively. The good fit to the experimental data indicates that the two confined hole states exhibit almost pure heavy- and light-hole characters. The simplest QD picture that emerges from these findings is depicted in Fig. 2(d), for which only one twofold degenerate confined QD state exists for each semiconductor carrier species (electron and heavy and light holes).

The obtained result of nearly pure heavy- and light-hole states in the QD is consistent with previous photocurrent²⁰ and absorption⁶ studies on SK QD ensembles embedded in waveguide structures, which reported strong heavy-hole character for the lowest QD valence band states. The resemblance of the QD polarization properties with those of a QW implies a large aspect ratio of the QD shape. The small energy separation between the heavy and light-hole states re-

sults from the VQWR, which predominantly affects the confinement energy of the light-hole due to its vertical elongation.

In conclusion, the polarization anisotropy of a pyramidal QD system, consisting of lens-shaped QDs connected to QWRs, has been investigated. The high in-plane symmetry (C_{3v}) of the present QD system was evidenced by isotropic in-plane linear polarization dependence. However, a very strong but different linear polarization anisotropy is observed for closely spaced QD transitions (< 7 meV) when the emission is extracted from a cleaved edge of the sample. The results are discussed in terms of the valence band structure and indicate nearly pure heavy- and light-hole states in the QD. This effect is attributed to the large aspect ratio of the QD shape. Moreover, for the particular system studied here the QD ground emission has a unique major direction of linear polarization, different from the emissions related to excited states and the VQWR barrier. This makes it possible to selectively couple the ground emission to an optical cavity. Further investigations are needed to clarify the impact of the C_{3v} symmetry on the exciton fine-structure splitting and photon entanglement applications.

The authors acknowledge fruitful discussions with Marc-André Dupertuis and Fabienne Michelini.

¹D. Gammon, E. S. Snow, B. V. Shanabrook, D. S. Katzer, and D. Park, Phys. Rev. Lett. **76**, 3005 (1996).

²V. D. Kulakovskii, G. Bacher, R. Weigand, T. Kümmell, A. Forchel, E. Borovitskaya, K. Leonardi, and D. Hommel, Phys. Rev. Lett. **82**, 1780 (1999).

³M. Bayer, G. Ortner, O. Stern, A. Kuther, A. A. Gorbunov, A. Forchel, P. Hawrylak, S. Fafard, K. Hinzer, T. L. Reinecke, S. N. Walck, J. P. Reithmaier, F. Kloppe, and F. Schäfer, Phys. Rev. B **65**, 195315 (2002).

⁴I. Favero, G. Cassabois, A. Jankovic, R. Ferreira, D. Darson, C. Voisin, C. Delalande, Ph. Roussignol, A. Badolato, P. M. Petroff, and J. M. Gerard, Appl. Phys. Lett. **86**, 041904 (2005).

⁵P. Yu, W. Langbein, K. Leosson, J. M. Hvam, N. N. Ledentsov, D. Bimberg, V. M. Ustinov, A. Y. Egorov, A. E. Zhukov, A. F. Tsatsul'nikov, and Y. G. Musikhin, Phys. Rev. B **60**, 16680 (1999).

⁶S. Cortez, O. Krebs, P. Voisin, and J. M. Gérard, Phys. Rev. B **63**, 233306 (2001).

⁷P. Jayavel, H. Tanaka, T. Kita, O. Wada, H. Ebe, M. Sugawara, J. Tatebayashi, Y. Arakawa, Y. Nakata, and T. Akiyama, Appl. Phys. Lett. **84**, 1820 (2004).

⁸P. Yu, W. Langbein, K. Leosson, J. M. Hvam, N. N. Ledentsov, D. Bimberg, V. M. Ustinov, A. Y. Egorov, A. E. Zhukov, A. F. Tsatsul'nikov, and Y. G. Musikhin, Phys. Rev. B **60**, 16680 (1999).

⁹R. M. Stevenson, R. J. Young, P. See, C. E. Norman, A. J. Shields, P. Atkinson, and D. A. Ritchie, Appl. Phys. Lett. **87**, 133120 (2005).

¹⁰M. H. Baier, S. Watanabe, E. Pelucchi, and E. Kapon, Appl. Phys. Lett. **84**, 1943 (2004).

¹¹M. H. Baier, C. Constantin, E. Pelucchi, and E. Kapon, Appl. Phys. Lett. **84**, 1967 (2004).

¹²G. Bester and A. Zunger, Phys. Rev. B **71**, 045318 (2005).

¹³A. Hartmann, Y. Ducommun, K. Leifer, and E. Kapon, J. Phys.: Condens. Matter **11**, 5901 (1999).

¹⁴M. H. Baier, A. Malko, E. Pelucchi, D. Y. Oberli, and E. Kapon, Phys. Rev. B **73**, 205321 (2006).

¹⁵K. F. Karlsson, E. S. Moskalenko, P. O. Holtz, B. Monemar, W. V. Schoenfeld, J. M. Garcia, and P. M. Petroff, Appl. Phys. Lett. **78**, 2952 (2001).

¹⁶A. Hartmann, Y. Ducommun, E. Kapon, U. Hohenester, and E. Molinari, Phys. Rev. Lett. **84**, 5648 (2000).

¹⁷F. Vouilloz, D. Y. Oberli, M.-A. Dupertuis, A. Gustafsson, F. Reinhardt, and E. Kapon, Phys. Rev. Lett. **78**, 1580 (1997).

¹⁸U. Bockelmann and G. Bastard, Phys. Rev. B **45**, 1688 (1992).

¹⁹G. Bastard, *Wave Mechanics Applied to Semiconductor Heterostructures* (Les Editions de Physique, Les Ulis, France, 1988), Chap. VII.

²⁰L. Chu, M. Arzberger, A. Zrenner, G. Böhm, and G. Abstreiter, Appl. Phys. Lett. **75**, 2247 (1999).